Chemistry & Biology, Vol. 11, 47–55, January, 2004, ©2004 Elsevier Science Ltd. All rights reserved. DOI 10.1016/j.chembiol.2003.12.016

Site-Specific Incorporation of a Photo-Crosslinking Component into RNA by T7 Transcription Mediated by Unnatural Base Pairs

Michiko Kimoto,[1] Masayuki Endo,[1] Tsuneo Mitsui,[2] Taeko Okuni,[1] Ichiro Hirao,[1,2,*] and Shigeyuki Yokoyama[1,3,4,*]

[1]Protein Research Group
RIKEN Genomic Sciences Center
1-7-22 Suehiro-cho
Tsurumi-ku, Yokohama
Kanagawa 230-0045

[2]Research Center for Advanced Science and Technology
The University of Tokyo
4-6-1 Komaba
Meguro-ku, Tokyo 153-8904

[3]Department of Biophysics and Biochemistry
Graduate School of Science
The University of Tokyo
7-3-1 Hongo, Bunkyo-ku
Tokyo 113-0033

[4]RIKEN Harima Institute at SPring-8
1-1-1 Kouto, Mikazuki-cho
Sayo, Hyogo 679-5148
Japan

Summary

A photo-sensitive ribonucleotide of 5-iodo-2-oxo(1H) pyridine (Iy) capable of site-specific incorporation into transcripts was developed. The site-specific Iy incorporation into RNA was achieved by T7 transcription mediated by unnatural base pairing between Iy and its partner, 2-amino-6-(2-thienyl)purine (s). By this specific transcription, Iy was incorporated into an anti-(Raf-1) RNA aptamer, which binds to human Raf-1 and inhibits the interaction between Raf-1 and Ras. Protein-dependent photo-dimerization of the aptamer was observed when Iy was located at specific positions in the aptamer, showing that the site-specific incorporation of the photo-sensitive component into RNA achieves highly specific crosslinking. This specific transcription mediated by the unnatural base pair would be a powerful tool for generating high-affinity RNA ligands and for analyzing RNA-RNA and RNA-protein interactions, as well as for constructing RNA-based nanostructures.

Introduction

Transcription that enables the site-specific incorporation of unnatural components into RNA facilitates the development of RNA molecules with novel functionality [1, 2]. This specific transcription is achieved by the third base pair working with the natural A-T(U) and G-C base pairs in transcription. The unnatural base pair can mediate the site-specific incorporation of the functional components carried by nucleoside triphosphates of the unnatural base. In comparison to the conventional methods using modified ribonucleotides in place of one of the natural ribonucleotides [2–10], such as 5-substituted uracil nucleotides, or by chemical RNA synthesis, the specific transcription would be a more powerful tool for generating RNA catalysts and ligands with high specificity and functionality, for site-specific labeling, and for creating immobilizing RNAs.

Until recently, the isoguanine-isocytosine (isoG-isoC) and xanthosine-diaminopyrimidine pairs were the only unnatural base pairs functioning with the natural base pairs in transcription [11, 12]. For example, the substrate of isoG was specifically incorporated into RNA by T7 RNA polymerase opposite isoC in templates. Using this base pair system, the site-specific incorporation of the 6-aminohexyl derivative of isoG into a small RNA fragment (10-mer) was performed [13]. Although the 6 position of isoG is an appropriate site for connecting with functional groups, a more suitable site is the 5 position of pyrimidines and their analogs. Many 5-substituted pyrimidines and the analogs can be synthesized via 5-halo derivatives [3, 6, 7, 10, 14–22]. In addition, since the 5 position does not take part in the base pair formation, the transcription efficiency for the incorporation of the 5-substituted pyrimidines is relatively high [6, 18]. Thus, the site-specific incorporation of isoC or diaminopyrimidine derivatives into RNA might serve many uses. However, the substrates of these 2-aminopyrimidines cannot be incorporated into RNA [11] because they lack the 2-keto group, which is important for recognition by T7 RNA polymerase [23]. Therefore, the further development of unnatural base pairs to which functional groups are easily introduced enables the creation of various RNA molecules with increased functionality.

We recently developed unnatural base pairs between 2-amino-6-*N,N*-dimethylaminopurine (**x**) and 2-oxo(1H) pyridine (**y**), and 2-amino-6-(2-thienyl)purine (**s**) and **y** [24–27], which were designed by combining the concepts of hydrogen-bonding patterns [12] and shape complementarity (Figure 1) [28, 29]. The **x**-**y** and **s**-**y** pairs worked with the natural A-T(U) and G-C base pairs in transcription [25, 27]. The substrate of **y** (yTP) was site specifically incorporated into RNA opposite **s** or **x** in templates by T7 RNA polymerase. In particular, the transcriptional specificity of the **s**-**y** pairing was as high as those of the natural base pairings, and the **s**-**y** pair was utilized in a cell-free transcription-translation system for the site-specific incorporation of an amino acid analog into a protein [27]. Thus, the nucleoside substrates of 5-substituted **y** would be useful for the specific transcription to prepare RNA molecules with novel functionality. In addition, the site-specific incorporation of heavy atoms, such as iodine and bromine, into RNA would facilitate X-ray crystallography of large RNA molecules and RNA-protein complexes. Here, we report the synthesis of the nucleoside 5′-triphosphate of 5-iodo-2-oxo(1H)pyridine (**Iy**), which has the potential to function as a photoactivated crosslinking component as well as an intermediate for further modification of the 5 position.

*Correspondence: hirao@mkomi.rcast.u-tokyo.ac.jp (I.H.); yokoyama@biochem.s.u-tokyo.ac.jp (S.Y.)

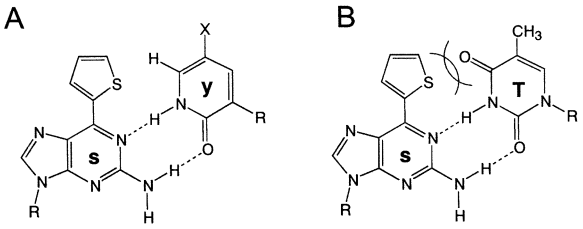

Figure 1. Unnatural Base Pairs between 2-Amino-6-(2-Thienyl)Purine (**s**) and 2-Oxo(1H)Pyridine (**y**: X = H) Derivatives (**Iy**: X = iodo) in Comparison with a Noncognate **s**-T Pair

The bulky 6-thienyl group of **s** prevents the noncognate **s**-T (B) and **s**-C pairings, but the relatively small hydrogen at the 6-position of **y** maintains the shape complementarity of the **s**-**y** and **s**-**Iy** pairings (A).

To examine the crosslinking ability, we performed the specific incorporation of **Iy**TP into an RNA ligand (so-called aptamer).

Results and Discussion

The ribonucleoside of 5-iodo-2-oxo(1H)pyridine (**Iy**) was derived from the ribonucleoside of **y** (Figure 2). The iodination of the nucleoside of **y** was accomplished by heating at 100°C for 12 hr with a mixture of iodine and potassium iodide under alkaline conditions [30] to give the nucleoside of **Iy** (34%). Although the yield was relatively low, the unreacted nucleoside of **y** (53%) was recovered from the reaction mixture. The product [3-(β-D-ribofuranosyl)-5-iodo-2-oxo(1H)pyridine] was characterized by ^{1}H-NMR, ^{13}C-NMR, and mass spectrometry. The ^{1}H-NMR spectrum of the base moiety indicated the introduction of iodine to the 5-position of **y**; the H5 signal (6.21 ppm, t, 1H, J = 6.8 Hz) of **y** had disappeared, and the chemical shifts of the H6 and H4 protons had changed from 7.58 ppm and 7.32 ppm to 7.77 ppm and 7.58 ppm, respectively. The UV spectrum of the **Iy** nucleoside displayed an absorption maximum of 318 nm, which was shifted from that of **y** (λ_{max} = 300 nm). The nucleoside of **Iy** (1 mM) in 10 mM Tris-HCl (pH 7.6) was completely decomposed ($t_{1/2}$ = 12 min) by irradiation at 302 nm for 1 hr, suggesting the potential of **Iy** as a crosslinking reagent. The ribonucleoside was converted to the nucleoside 5′-triphosphate (**Iy**TP) to function as a substrate in T7 transcription. The molar absorption coefficient of **Iy**TP (1.2×10^3 at 260 nm and 5.5×10^3 at 318 nm) at pH 7.0 was determined by quantitative analysis of the phosphorus in the compound [31].

First, the specific incorporation of **Iy**TP into RNA was assessed using short DNA templates (35-mer, temp35**s** containing an unnatural **s** base and temp35A consisting of the natural bases as a control) from which 17-mer transcripts were obtained. The 35-mer template strands included the promoter sequence for T7 RNA polymerase followed by a short sequence consisting of C and T, except for **s** or A at position +11, and G at position +16 (Figure 3A). These template strands were annealed with a 21-mer nontemplate strand, and the transcription was carried out by T7 RNA polymerase with 1 mM natural NTPs, 10 mM GMP, and 0.1 μCi/μl [α-^{32}P]ATP in the presence or absence of **Iy**TP (0, 0.25, 0.5, or 1 mM) at 37°C for 3 hr. The nucleotides that became the 5′ neighbor of A in the products were labeled at the 3′ phosphates, because [α-^{32}P]ATP was used for internal labeling in transcription (Figure 3A). Then, the transcripts were digested with RNase T_2, and the resulting labeled nucleoside 3′ monophosphates, including the nucleotide opposite **s**, were analyzed by 2D thin-layer chromatography (2D-TLC) [25, 27] (Figure 3B and Table 1, entries 1–7).

The nucleotide composition analysis of the transcripts confirmed the specific incorporation of **Iy** into RNA opposite **s** in the templates (Figure 3B and Table 1). On the 2D-TLC, a spot corresponding to the nucleotide of **Iy** (**Iy**p) appeared only from the transcription using temp35**s** (Figure 3B). Quantification of the spots on the 2D-TLC indicated that the incorporation efficiency of **Iy**TP was higher than that of **y**TP [27]; the combination of 0.25 mM **Iy**TP with 1 mM natural NTPs was sufficient for the specific **Iy**TP incorporation opposite **s** (Table 1, entry 7). This high efficiency resulted in the subtle misincorporation of **Iy**TP opposite natural bases in the templates, when the concentration (1 mM) of **Iy**TP was equivalent to those of the natural NTPs (1 mM) (Table 1, entry 1). The specificity was improved by decreasing the concentration (0.25 mM) of **Iy**TP (Table 1, entries 3 and 7). In this assay, the composition of Gp was relatively small in comparison to the theoretical number. However, this did not result from the **s**-**y** pairing in transcription, because this tendency also appeared in the natural transcription using the control template, temp35A, in the absence of **Iy**TP (Table 1, entry 4).

Next, we incorporated **Iy** into an RNA aptamer to examine the photo-crosslinking ability of the RNA aptamer in the presence of its target molecule. For this purpose, we chose an anti-(Raf-1) aptamer (100-mer), which was obtained by in vitro selection as an RNA ligand that binds to the human Raf-1 protein and inhibits the interaction between Raf-1 and Ras [32]. Enzymatic and chemical experiments indicated that the aptamer forms a psuedoknot-type structure (Figure 4A) [32]. The substrate, **Iy**TP, was incorporated within specific positions (positions 84, 87, 92, or 84 and 92) of the 3′ single-stranded region of the aptamer (Figure 4A). The site-specific incorporation of **s** into DNA templates can be achieved by PCR amplification using 3′ primers containing **s** at specific positions (Figure 4B). The internally labeled transcripts obtained by T7 transcription in the presence or absence of **Iy**TP were analyzed by gel electrophoresis (Figure 4C). In consideration of the high effi-

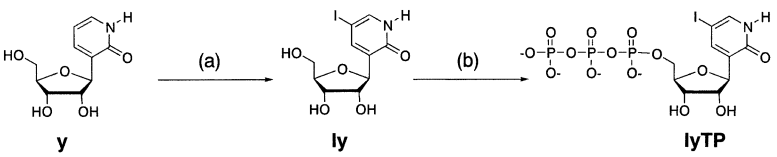

Figure 2. Synthesis of **Iy**TP

Conditions: (a) I_2, KI, Na_2CO_3, H_2O, (b) $POCl_3$, proton sponge in $PO(OCH_3)_3$, and then tri-*n*-butylamine, bis(tributylammonium)pyrophosphate in DMF.

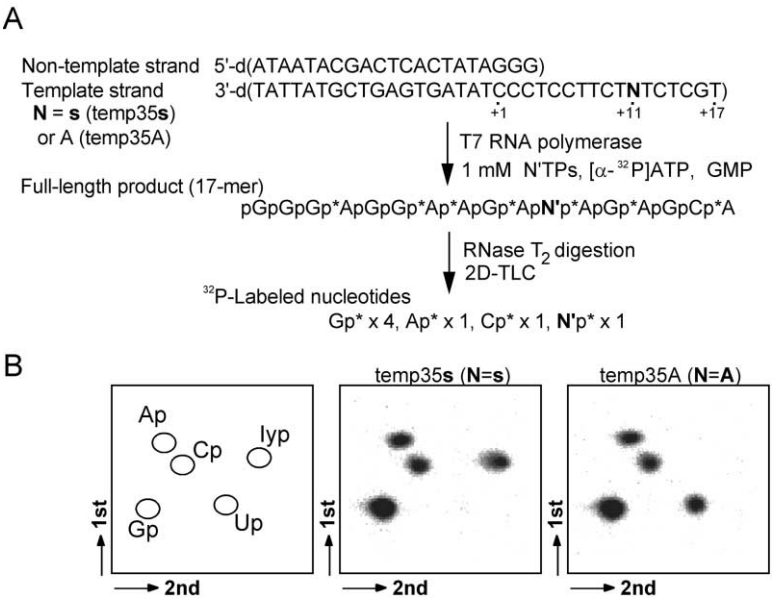

Figure 3. T7 Transcription Employing the s-Iy Pairing

Schemes of the experiments (A) and two-dimensional TLC (B) for nucleotide-composition analyses of transcripts. The quantitative data are shown in Table 1, entries 1–7.

ciency of IyTP, the transcription was carried out with 0.25 mM IyTP and 1 mM natural NTPs. The relative yields of the transcripts containing one Iy nucleotide at position 84, 87, or 92 (Figure 4C, lanes 4, 6, and 8, respectively) were 56%–69% as compared to that of the natural transcript from the original template (Figure 4C, lane 1). Even in the transcription using the template containing two s bases (Figure 4C, lane 10), the transcript containing two Iy nucleotides was obtained with a 33% yield relative to the natural transcript. The transcription efficiencies in the absence of IyTP were lower than those in the presence of IyTP, and the transcriptions were partially paused at the positions opposite s in the templates (Figure 4C, lanes 3, 5, 7, and 9).

The site-specific incorporation of IyTP into the aptamer was confirmed by the nucleotide composition

Table 1. Nucleotide Composition Analysis of T7 Transcripts

Entry	Template	[α-32P] NTP	IyTP (mM)	Composition of Nucleotides Incorporated as 5′ Neighbor of A or G				
				Ap[a]	Gp	Cp	Up	Iyp
1	temp35A	ATP	1	1.02[b] [1][c] (0.03)[d]	0.94 [1] (0.01)	3.99 [4] (0.02)	1.03 [1] (0.01)	0.02 [0] (0.01)
2	temp35A	ATP	0.5	1.03 [1] (0.02)	0.94 [1] (0.01)	3.98 [4] (0.02)	1.04 [1] (0.02)	0.01 [0] (0.01)
3	temp35A	ATP	0.25	1.05 [1] (0.04)	0.94 [1] (0.02)	3.96 [4] (0.05)	1.05 [1] (0.02)	<0.01 [0] (<0.01)
4	temp35A	ATP	0	1.04 [1] (0.02)	0.92 [1] (0.02)	4.00 [4] (0.01)	1.04 [1] (0.02)	ND[e]
5	temp35s	ATP	1	1.05 [1] (0.02)	0.92 [1] (0.02)	4.04 [4] (0.04)	0.02 [0] (0.01)	0.98 [1] (0.02)
6	temp35s	ATP	0.5	1.06 [1] (0.02)	0.93 [1] (0.01)	3.99 [4] (0.01)	0.03 [0] (0.01)	0.99 [1] (0.03)
7	temp35s	ATP	0.25	1.05 [1] (0.01)	0.93 [1] (0.01)	4.02 [4] (0.01)	0.03 [0] (0.01)	0.97 [1] (0.01)
8	temp119	ATP	0	6.03 [6] (0.13)	5.86 [6] (0.13)	7.06 [7] (0.04)	6.06 [6] (0.15)	ND
9	temp119	ATP	0.25	6.06 [6] (0.17)	5.87 [6] (0.18)	6.86 [7] (0.12)	6.13 [6] (0.14)	0.10 [0] (0.03)
10	temp119	GTP	0	7.94 [8] (0.09)	4.92 [5] (0.02)	4.11 [4] (0.09)	5.03 [5] (0.06)	ND
11	temp119	GTP	0. 25	7.85 [8] (0.09)	4.94 [5] (0.14)	4.13 [4] (0.12)	5 .00 [5] (0.26)	0.08 [0] (0.03)
12	temp119s84	ATP	0.25	5.97 [6] (0.13)	5.84 [6] (0.15)	7.03 [7] (0.01)	6.06 [6] (0.17)	0.11 [0] (0.04)
13	temp119s84	GTP	0.25	7.97 [8] (0.16)	5.01 [5] (0.10)	3.05 [3] (0.11)	5.04 [5] (0.11)	0.93 [1] (0.03)
14	temp119s87	ATP	0.25	6.01 [6] (0.24)	5.83 [6] (0.17)	6.08 [6] (0.17)	6.05 [6] (0.25)	1.04 [1] (0.01)
15	temp119s87	GTP	0.25	7.83 [8] (0.11)	4.86 [5] (0.15)	4.10 [4] (0.10)	5.13 [5] (0.27)	0.09 [0] 0.04
16	temp119s92	ATP	0.25	5.12 [5] (0.20)	5.94 [6] (0.13)	7.01 [7] (0.21)	5.85 [6] (0.14)	0.08 [0] (0.03)
17	temp119s92	GTP	0.25	7.04 [7] (0.13)	5.00 [5] (0.03)	4.19 [4] (0.08)	4.85 [5] (0.05)	0.95 [1] (0.04)
18	temp119s84s92	ATP	0.25	5.07 [5] (0.02)	5.73 [6] (0.03)	6.82 [7] (0.22)	6.28 [6] (0.26)	0.13 [0] (0.01)
19	temp119s84s92	GTP	0.25	7.02 [7] (0.12)	4.94 [5] (0.13)	3.08 [3] (0.09)	5.05 [5] (0.14)	1.92 [2] (0.12)

Transcription was carried out using a solution (20 μl) containing 2 μM of template for temp35A and temp35s or ~0.13 μM of template for the temp119 series, 1 mM each natural NTP, 2 μCi of [α-32P]ATP or [α-32P]GTP, 10 mM GMP, and 50 units of T7 RNA polymerase at 37°C for 3–6 hr.

[a] Composition of nucleotides incorporated as 5′ neighbor of p*A or p*G, as shown in Figures 2 and 3.

[b] The values were determined using the following formula: (radioactivity of each nucleotide)/[total radioactivity of all nucleotides (3′-monophosphates)] × (total number of nucleotides at 5′ neighbor of A or G).

[c] The theoretical number of each nucleotide is shown in brackets.

[d] Standard deviations are shown in parentheses.

[e] Not detected.

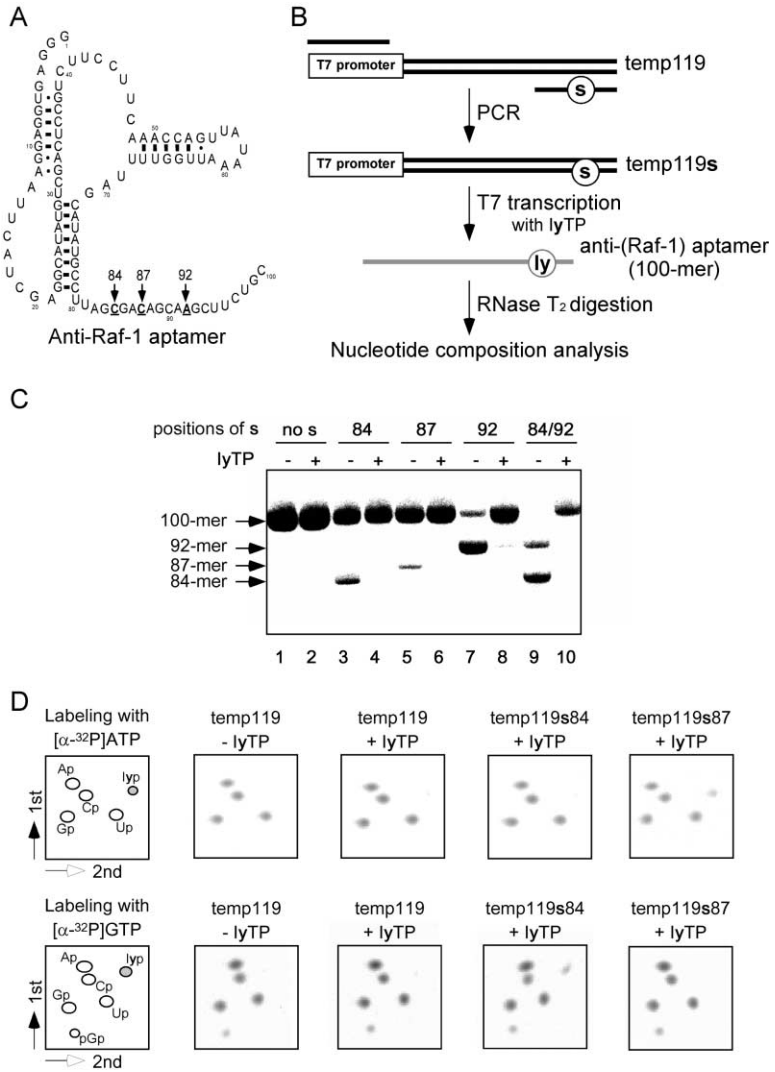

Figure 4. Site-Specific ly Incorporation into the Anti-(Raf-1) RNA Aptamer by T7 Transcription

(A) The secondary structure of the anti-(Raf-1) aptamer. The bases at positions 84, 87, and 92 for the site-specific ly incorporation are in bold, underlined type.

(B) Schemes of the T7 transcription. The templates containing s at specific positions (temp119s84, s87, s92, and s84s92) were generated from a plasmid encoding the T7 promoter and the anti-(Raf-1) aptamer sequence by PCR using a 5′ primer including the T7-promoter sequence and a 3′ primer containing s.

(C) Gel electrophoresis of transcripts obtained by using [α-^{32}P]ATP and templates lacking s (lanes 1 and 2; temp119) or containing s at positions 84 (lanes 3 and 4; temp119s84), 87 (lanes 5 and 6; temp119s87), 92 (lanes 7 and 8; temp119s92), or 84 and 92 (lanes 9 and 10; temp119s84s92) in the presence or absence of lyTP (0.25 mM).

(D) Two-dimensional TLC for nucleotide-composition analyses of transcripts labeled with [α-^{32}P]ATP or [α-^{32}P]GTP. The quantitative data are shown in Table 1, entries 8–19.

analysis (Figure 4D and Table 1, entries 8–19). Transcripts were labeled internally with [α-^{32}P]ATP or [α-^{32}P]GTP, because the insertion positions of ly were located at the 5′ side of either A or G. When the transcripts were labeled with [α-^{32}P]GTP, guanosine 3′,5′-diphosphate (pGp) was generated from the 5′ terminal guanosine of the transcripts, and the spot corresponding to pGp was observed on 2D-TLC. As shown in Figure 4D, a high specificity of ly incorporation was observed in the 2D-TLC; the transcript from temp119s84 yielded a spot corresponding to the nucleoside 3′ phosphate of ly (lyp) only by labeling with [α-^{32}P]GTP, and the transcript from temp119s87 gave the spot corresponding to lyp only by labeling with [α-^{32}P]ATP. Furthermore, quantification of the TLC spots also showed the site-specific ly incorporation into the transcripts opposite s in the templates (Table 1, entries 12–19). A few ly misincorporations into the aptamers opposite natural bases in the templates were observed (Table 1, entries 9, 11, 12, 15, 16, and 18), and the values of the ly composition in the transcripts were 0.08–0.13. However, these misincorporations correspond to only 0.3%–0.6% per position in the transcripts as determined by the following formula: (the ly composition)/(total numbers of nucleotide at 5′ neighbor of A or G) × 100 (%).

Photo-crosslinking of the anti-(Raf-1) aptamers containing ly at specific positions was performed by irradiation at 312 nm for 1 hr at 4°C in the presence of GST-RBD, the Ras binding domain of Raf-1 as a fusion form with glutathione S-transferase [33]. Prior to irradiation, these aptamers were 5′ labeled with [γ-^{32}P]ATP, and then after irradiation the products were analyzed by gel electrophoresis (Figure 5A). We observed that the aptamers containing ly at position 84 (aptamer ly84) or 87 (aptamer ly87) gave a clear band corresponding to a photo-crosslinked product (Figure 5A, lanes 6 and 8). In contrast, the photo-crosslinking of the aptamers containing ly at position 92 or positions 84 and 92 (Figure 5A, lanes 10 and 12) was much less efficient than those at position 84 or 87. The photo-crosslinking of the non-modified aptamers comprising only the natural bases (Figure 5A, lanes 2 and 4) or the aptamer containing 5-iodouridines (IU) in place of uridines at random positions, which was prepared by a conventional method

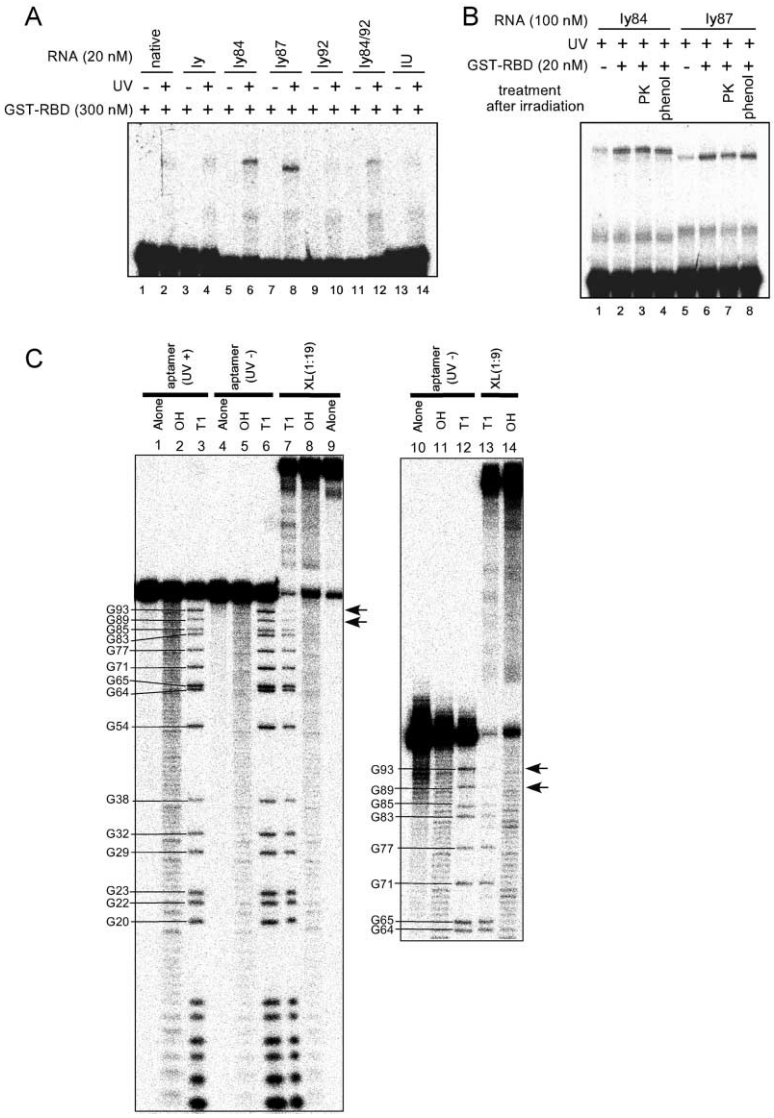

Figure 5. Photo-Crosslinking Experiments of the Anti-(Raf-1) Aptamers Containing Iy at Specific Positions

(A) Photo-crosslinking was performed by using RNAs transcribed from the original template (temp119) lacking s with four natural NTPs (native), from the original template with the natural NTPs (1 mM) and IyTP (0.25 mM) (Iy), from the templates containing s at the specific positions with the natural NTPs (1 mM) and IyTP (0.25 mM) (Iy84, Iy87, Iy92, and Iy84/92), and from the original template with the natural NTPs (1 mM) and 5-iodoUTP (0.4 mM) (IU). The RNAs Iy84, Iy87, Iy92, and Iy84/92 were obtained from the templates temp119s84, temp119s87, temp119s92, and temp119s84/92, respectively. Prior to UV irradiation, solutions containing the ^{32}P-labeled RNA (20 nM) and GST-RBD (300 nM) were incubated at 37°C for 30 min to form the RNA:GST-RBD complexes. The solutions were then irradiated by using a 312 nm transilluminator on ice for 1 hr. Products were detected on an 8% polyacrylamide gel with 7 M urea for analysis.

(B) Analysis of the crosslinked products. After UV irradiation, the solutions were incubated with proteinase K (PK) or extracted with phenol/$CHCl_3$ (phenol).

(C) RNase T1 mapping. The autoradiograms show the partially digested fragments of the 5′-end-labeled crosslinked or uncrosslinked RNAs. Enzymatic probing: alone, RNA in the RNase T1 reaction buffer only; OH, alkaline hydrolysis; T1, RNase T1. RNA: XL(1:19), the crosslinked product between the 5′-end-labeled aptamer comprising only the natural bases (wt*) and the nonlabeled aptamer Iy87 (molar ratio in the crosslinking reaction, wt*:Iy87 = 1:19); XL(1:9), the crosslinked product between wt* and the nonlabeled Iy87 (molar ratio in the crosslinking reaction, wt*:Iy87 = 1:9); aptamer (UV+), the gel-purified wt* after UV irradiation; aptamer (UV−), wt* without UV irradiation. Arrows mark positions 89 and 93, highlighting the photo-crosslinking sites.

[34], was also inefficient (Figure 5A, lane 14). These results indicate that the site-specific Iy incorporation into the aptamer is important for photo-crosslinking.

To identify the photo-crosslinked product of the aptamer, we did further experiments using the aptamers Iy84 and Iy87. The photo-crosslinked products were also obtained by the reaction of the aptamers in the absence of GST-RBD, although the efficiency was much lower than that in the presence of GST-RBD (Figure 5B, lanes 1 and 5). After the treatments of the photo-crosslinked product with proteinase K or phenol (Figure 5B, lanes 3, 4, 7, and 8), no change of the band was observed on the gel. Thus, these results indicate that the product was not generated by crosslinking between the aptamer and the protein. The mobility of the product band on the gel was close to that of a 200-mer oligoribonucleotide (data not shown). Therefore, we concluded that the photo-crosslinked product was obtained by dimerization of the aptamer.

We then determined the photo-crosslinking sites of the aptamer Iy87 by RNase T1 mapping. For this mapping, the photo-crosslinking was performed in the presence of GST-RBD with the mixture of the 5′-^{32}P-labeled aptamer comprising only the natural bases (wt*) and the nonlabeled aptamer Iy87. The photo-crosslinked dimer between wt* and Iy87 was purified by gel electrophoresis and was partially digested with RNase T1. The digested products were analyzed by denaturing gel electrophoresis (Figure 5C). The digested fragments containing nucleotides crosslinked to Iy87 were expected to appear as bands migrating more slowly than the uncrosslinked fragments on the gel. As shown in Figure 5C, the intensities of the bands corresponding to the fragments 1-83 (G83), 1-85 (G85), especially 1-89 (G89), and 1-93 (G93) of the photo-crosslinked dimer (Figure 5C, lanes 7 and 13) were much lower than those of uncrosslinked RNAs (Figure 5C, lanes 3, 6, and 12). No clear differences in the band intensities were observed between lanes 1–3 and lanes 4–6, which were derived from wt* with and without UV irradiation, respectively.

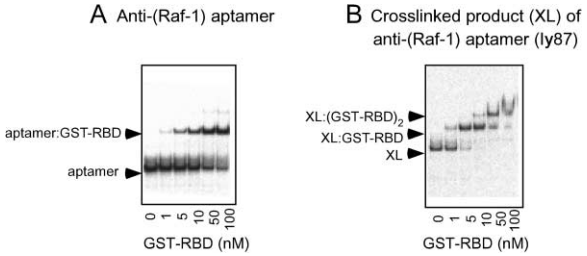

Figure 6. Gel Mobility-Shift Assays

Binding of the anti-(Raf-1) aptamer with GST-RBD (A) and the crosslinked product of Iy87 with GST-RBD (B). Approximately 10 nM of the anti-(Raf-1) aptamer or the crosslinked product of aptamer Iy87 (XL) was applied with 0–100 nM GST-RBD on a native gel. The bands corresponding to the anti-(Raf-1) aptamer, the aptamer:GST-RBD (1:1) complex, XL, the XL:GST-RBD (1:1) complex, and the XL:(GST-RBD)$_2$ (1:2) complex are indicated on the left.

Thus, the lower intensities of the G83, G85, G89, and G93 bands in lanes 7 and 13 depend on the photo-crosslinking with the aptamer Iy87.

RNase T1 mapping indicated that the crosslinking sites of Iy87 are located near the 3′ single-stranded region of the aptamer at positions around 83–100. This is quite consistent with the aptamer structure and function; the region from positions 1–80 formed the pseudoknot structure, and the region from positions 81–100 was neither involved in folding nor important for binding to GST-RBD (Figure 4A) [32]. In fact, no photo-crosslinked product was observed from the crosslinking of the nonlabeled aptamer Iy87 with the ^{32}P-labeled 1–80 fragment of the aptamer comprising only the natural bases (aptamer Iy87:1–80 fragment = 9:1 molar ratio) in the presence of GST-RBD (data not shown). These results support the photo-crosslinking at the 3′ single-stranded region of the aptamers.

This dimerization of the aptamers was stimulated in the presence of the protein. This may be a consequence of the protein dimerization; the GST moiety of the protein is apt to dimerize in solution [35], and this allows the two aptamers, each bound to the RBD moiety, to approach each other. Conversely, the photo-crosslinked dimer of the aptamer was expected to bind to two molecules of GST-RBD. Indeed, efficient complex formation between the crosslinked aptamer and the two GST-RBD molecules was observed by a gel-shift assay (Figure 6B). The (1:1) complex between the ordinary anti-(Raf-1) aptamer and the GST-RBD was observed on the gel (Figure 6A). In contrast, the crosslinked aptamer (10 nM) easily formed the (1:2) complex with an excess amount of GST-RBD (>10 nM) (Figure 6B). This indicates that the photo-crosslinking does not disturb the binding of the dimer aptamer with the protein, supporting the crosslinking between the aptamers at their 3′-terminal regions.

The photo-crosslinking of the anti-(Raf-1) aptamers containing Iy at specific positions shows that such photo-crosslinking would be useful for analyzing the quaternary structures of proteins. The crosslinked dimer-aptamer could be used as a scaffold for promoting the dimerization of proteins and for constructing RNA-based nanostructures [36–38]. In addition, RNA photo-crosslinking experiments can provide meaningful information for RNA association into more complex, higher-ordered structures. For example, in ϕ29 viral procapsid formation, the distance information obtained by the site-specific photo-crosslinking of the multiplex of DNA-packaging RNA (pRNA) was used as constraints in computer modeling of the three-dimensional structure of the pRNA complex [39].

At present, RNA aptamers with photo-crosslinking ability (photoaptamers) have been prepared by transcription using 5-iodouridine triphosphate in place of UTP, and thus all of the uridines in the aptamers are substituted with 5-iodouridine [8, 9, 40, 41]. Photoaptamers can form a specific covalent bond with their target molecules, and nonspecific binding can be reduced by stringent washing of the complexes. In comparison to this conventional method, the site-specific incorporation of the photo-crosslinking component into aptamers could increase the specificity to the target molecules by site-specific crosslinking and reduce the aptamer damage caused by an excess of photo-sensitive components in the aptamers. To develop efficient RNA aptamers that can covalently crosslink with a target molecule, we are currently carrying out in vitro selections of RNA photoaptamers containing Iy.

Significance

The photo-sensitive component, 5-iodo-2-oxo(1H)pyridine (Iy), can be incorporated into RNA at desired positions by T7 transcription involving the unnatural s-y base pairing. The DNA templates containing s can be prepared by PCR using a 3′ primer containing s at the desired positions. Thus, this specific transcription is much easier than the chemical synthesis of RNA for preparing RNAs with novel functionality, and the transcripts might have more efficient and specific functionalities than those obtained by the random incorporations of functional components in place of the natural nucleotides. Here, we have shown the importance of the photo-sensitive component incorporation within specific positions in the RNA aptamer for effective crosslinking. RNAs containing the photo-sensitive Iy would be useful for the studies of RNA-RNA and RNA-protein interactions and for the tight binding of aptamers to target molecules by photo-crosslinking, toward diagnostic and therapeutic applications of RNA photoaptamers [40, 41]. In addition, the site-specific crosslinking between RNA molecules might be useful for constructing RNA-based nanostructures and could provide useful information about complex, higher-ordered structures [36–39]. The RNA molecules containing Iy at specific positions could also be used as rational phasing tools for X-ray crystallography of RNA molecules and RNA-protein complexes. Furthermore, a range of functional components can be derived chemically from Iy, and these could be also incorporated into RNA site specifically. Thus, the specific transcription mediated by the s-y pair should be a powerful tool for developing a wide range of novel functional RNAs.

Experimental Procedures

3-(β-D-ribofuranosyl)-2-oxo(1H)pyridine was synthesized according to a previously reported method [25, 42]. ^{1}H-NMR (270 MHz), ^{13}C-NMR (68 MHz), and ^{31}P-NMR (109 MHz) spectra were recorded on a JEOL EX270 magnetic resonance spectrometer. Purification of nucleosides was performed on a Gilson HPLC system with a preparative C18 column (Waters Microbond Sphere, 150 × 19 mm). Triphosphates were purified on a DEAE-Sephadex A-25 column (300 × 15 mm) followed by a Gilson HPLC system with an analytical column (Synchropak RPP, 250 × 4.6 mm, Eichrom Technologies). High resolution mass spectra (HRMS) and electrospray ionization mass spectra (ESI-MS) were recorded on a JEOL HX-110 mass spectrometer and a Waters ZMD 4000 LC/MS system, respectively.

Synthesis of 3-(β-D-Ribofuranosyl)-5-Iodo-2-Oxo(1H)Pyridine

A mixture of iodine (382 mg, 1.5 mmol) and potassium iodide (438 mg, 2.6 mmol) in water (12 ml) was added to a solution of 3-(β-D-ribofuranosyl)-2-oxo(1H)pyridine (228 mg, 1.0 mmol) in 0.1 M Na_2CO_3 (12 ml). The reaction mixture was stirred at 100°C for 12 hr in a sealed vessel. After cooling to room temperature, NH_4Cl (200 mg) was added to the reaction mixture. The solution was washed with CH_2Cl_2, and then the water layer was concentrated in vacuo. The product [3-(β-D-ribofuranosyl)-5-iodo-2-oxo(1H)pyridine, 118 mg, 34%] and the unreacted raw material [3-(β-D-ribofuranosyl)-2-oxo(1H)pyridine, 121 mg, 53%] were purified by reversed-phase HPLC with a gradient from 4% to 15% (6 min) and then 15% to 30% (6 min) CH_3CN in H_2O. ^{1}H-NMR (270 MHz, DMSO-d6): δ 11.90 (s, 1H), 7.77 (d, 1H, J = 2.4 Hz), 7.58 (d, 1H, J = 2.4 Hz), 5.12 (d, 1H, J = 4.3 Hz), 4.97 (t, 1H, J = 5.4 Hz), 4.73 (d, 1H, J = 4.9 Hz), 4.63 (d, 1H, J = 4.0 Hz), 3.80 (m, 3H), 3.61 (dd, 1H, J = 2.6, 12.4 Hz), 3.45 (dd, 1H, J = 3.5, 12.4 Hz). ^{13}C-NMR (68 MHz, DMSO-d6): δ 160.00, 143.83, 138.97, 132.88, 83.40, 80.26, 74.56, 70.46, 65.38, 61.06. HRMS (FAB, 3-NBA matrix) for $C_{10}H_{13}NO_5I$ (M + 1): calcd., 353.9838; found, 353.9844.

Synthesis of 3-(β-D-Ribofuranosyl)-5-Iodo-2-Oxo(1H)Pyridine 5′-Triphosphate

To a solution of 3-(β-D-ribofuranosyl)-5-iodo-2-oxo(1H)pyridine (35 mg, 0.1 mmol) and a proton sponge [43] (33 mg, 0.15 mmol) in trimethyl phosphate (500 μl), $POCl_3$ (12 μl, 0.13 mmol) was added at 0°C. The reaction mixture was stirred at 0°C for 5 hr. Tri-n-butylamine (120 μl, 0.5 mmol) was added to the mixture, followed by 0.5 M bis(tributylammonium)pyrophosphate in a DMF solution (1.0 ml, 0.5 mmol). After 5 min, the reaction was quenched by the addition of 0.5 M triethylammonium bicarbonate (TEAB, 500 μl). The resulting crude product was purified by DEAE Sephadex A-25 column chromatography (eluted by a linear gradient of 50 mM to 1 M TEAB) and then by C18-HPLC (eluted by a gradient of 0% to 30% CH_3CN in 100 mM triethylammonium acetate). ^{1}H-NMR (270 MHz, D_2O): δ 7.87 (s, 1H), 7.60 (s, 1H), 4.80 (d, 1H, J = 3.8 Hz), 4.03 (m, 5H), 3.03 (q, 18H, J = 7.3 Hz), 1.11 (t, 27H, J = 7.3 Hz). ^{31}P-NMR (109 MHz, D_2O): δ −10.34 (d, 1H, J = 20.1 Hz), −10.93 (d, 1H, J = 20.1 Hz), −22.89 (t, 1H, J = 20.1 Hz). ESI-MS for $C_{10}H_{14}INO_{14}P_3$ (M − 1): calcd., 591.87; found, 591.70.

Oligonucleotides

Oligodeoxynucleotides were synthesized by standard phosphoramidite chemistry on a DNA synthesizer (model 392, PE Applied Biosystems). PCR primers for the dsDNA encoding the anti-(Raf-1) RNA aptamer were as follows (T7 promoter region is underlined and **s** denotes 2-amino-6-(2-thienyl)purine): 39.45, 5′-GGTAATACGACTCACTATAGGGAGTGGAGGAATTCATCG; 29.45, 5′-GCAGAAGCTTGCTGTCGCTAAGGCATATG; 29.45s84, 5′-GCAGAAGCTTGCTGTCsCTAAGGCATATG; 29.45s87, 5′-GCAGAAGCTTGCTsTCGCTAAGGCATATG; 29.45s92, 5′-GCAGAAGCsTGCTGTCGCTAAGGCATATG; 29.45s84/92, 5′-GCAGAAGCsTGCTGTCsCTAAGGCATATG.

Preparation of Templates for T7 Transcription

Template DNAs for the anti-(Raf-1) RNA aptamer were amplified from the aptamer-encoding pCR II-TOPO vector, TOPO-9A [32], by PCR using a 5′-end primer (39.45) and a 3′-end primer (29.45, 29.45s84, 29.45s87, 29.45s92, or 29.45s84/92). PCR was carried out in 10 mM Tris-HCl buffer (pH 8.3) with 50 mM KCl, 1.5 mM $MgCl_2$, 0.2 mM each dNTP, 1 μM each primer, 1 ng/μl TOPO-9A digested by BamHI (Takara Shuzo) and 0.025 U/μl Taq DNA polymerase (Takara Shuzo) on a PTC-100 Program Thermal Controller (MJ Reseach, Inc., Waltham, MA). The conditions were 15 or 20 cycles of denaturation at 94°C for 0.5 min, primer annealing at 40°C for 0.5 min, and primer extension at 60°C for 1 min, followed by an incubation at 60°C for 5 min. The PCR products were extracted with phenol/chloroform, precipitated with ethanol, and then resuspended in 10 mM Tris-HCl buffer (pH 7.6) containing 10 mM NaCl.

T7 Transcription

The specific transcription employing the **s**-**Iy** pair was carried out on a 20 μl scale with 40 mM Tris-HCl buffer (pH 8.0) with 5 mM DTT, 24 mM $MgCl_2$, 2 mM spermidine, 0.01% Triton X-100, 10 mM GMP, 1 mM each NTP, 0-1 mM IyTP, 0.1 μCi/μl [α-^{32}P]ATP or [α-^{32}P]GTP, 4 μl of the template DNA, and 2.5 U/μl T7 RNA polymerase (Takara Shuzo) [25, 27]. After incubation for 3–6 hr at 37°C, the reaction was quenched by the addition of an equal volume of dye solution (10 M urea, 0.05% bromophenol blue). The mixture was heated at 75°C for 3 min and then loaded onto a 20% (for 17-mer RNAs) or 8% (for 100-mer RNAs) denaturing polyacrylamide gel containing 7 M urea. The transcripts on the gel were analyzed with a Bio-imaging analyzer (BAS-2500, Fuji Photo Film Co., Ltd., Tokyo).

Nucleotide Composition Analysis of T7 Transcripts

The nucleotide composition analysis of the transcripts was performed according to the literature [25, 27]. After purification by gel electrophoresis, the transcripts were digested by RNase T_2 (Sigma) (0.375 U/μl) in 15 mM sodium acetate buffer (pH 4.5) containing 1.5% glycerol at 37°C overnight. The digested products were analyzed by two-dimensional TLC, and the spots on the TLC plates were quantitated with the BAS-2500.

Photo-Crosslinking

Photo-crosslinking was carried out in 96-well microtiter plates using a 312-nm, broad-band UV transilluminator (TVC-312R/J; Spectronics Corp., Westbury, NY). RNA labeled with ^{32}P at the 5′ end (final 20 or 100 nM) was mixed with the Ras binding domain of Raf-1 fused with glutathione S-transferase (GST-RBD) (20 or 300 nM) in binding buffer (PBS with 5 mM $MgCl_2$, buffer A) containing 160 μg/ml bovine serum albumin (BSA, Sigma), 1 mM DTT, and 7.3% glycerol, and then the mixture was incubated for 30 min at 37°C. After the incubation, the reaction mixtures (40–120 μl) were placed on ice and were irradiated for 1 hr with the UV transilluminator at a distance of about 1 cm from the samples. The samples were covered with the polystyrene lid of the microtiter plate to shield them from wavelengths below 300 nm. After irradiation, the products were analyzed on an 8% polyacrylamide gel containing 7 M urea. Protease digestion of the crosslinked products was carried out by a treatment with 1 μg/ml of proteinase K for 1 hr at 65°C after irradiation.

RNase T1 Mapping

The anti-(Raf-1) aptamer labeled with ^{32}P at the 5′ end (wt*) was mixed with the nonlabeled aptamer **Iy**87 (molar ratio of wt*:**Iy**87 = 1:9 or 1:19) in buffer A. The RNA solution (200 nM) was incubated with an equal volume of the GST-RBD solution (200 nM) for 30 min at 37°C. Then, the solution was UV irradiated for 1 hr as described above. After irradiation, the RNAs were extracted with phenol/chloroform and precipitated with isopropyl alcohol. The crosslinked and uncrosslinked RNAs were then separated and purified by gel electrophoresis. Alkaline digestion was performed in 50 mM sodium carbonate (pH 9.0), 1 mM EDTA, and 0.25 mg/ml *E. coli* tRNA for 6 min at 90°C. RNase T1 digestion (0.1 unit/μl) was performed in 20 mM sodium citrate (pH 5.0), 7 M urea, 1 mM EDTA, 0.025% bromophenol blue, and 0.25 mg/ml *E. coli* tRNA for 12 min at 55°C. The digested samples were analyzed on an 8% polyacrylamide gel containing 7 M urea.

Gel Mobility-Shift Assay

The ^{32}P-labeled anti-(Raf-1) aptamer and the crosslinked products (approximately 0.8 pmol) in the binding buffer (20 μl) were mixed

with the binding buffer (20 μl) containing *Escherichia coli* tRNA (100 μg/ml, Sigma) and were left for 5 min at room temperature. An aliquot (5 μl) was mixed with the GST-RBD solution (0–200 nM, 5 μl) in the binding buffer containing 160 mg/ml BSA, 1 mM DTT, and 10% glycerol, and then the mixture was incubated for 30 min at 37°C. The RNA-protein interaction was analyzed by electrophoresis on a native 5% polyacrylamide gel (39:1) in 12.5 mM Tris-125 mM glycine buffer at room temperature.

Received: August 20, 2003
Revised: October 20, 2003
Accepted: October 22, 2003
Published: January 23, 2004

References

1. Benner, S.A., Burgstaller, P., Battersby, T.R., and Jurczyk, S. (1999). Did the RNA world exploit an expanded genetic alphabet? In The RNA World, R.F. Gesteland, T.R. Cech, and J.F. Atkins, eds. (Cold Spring Harbor, NY: Cold Spring Harbor Laboratory Press), pp. 163–181.
2. Vaish, N.K., Larralde, R., Fraley, A.W., Szostak, J.W., and McLaughlin, L.W. (2003). A novel, modification-dependent ATP-binding aptamer selected from an RNA library incorporating a cationic functionality. Biochemistry *42*, 8842–8851.
3. Verma, S., and Eckstein, F. (1998). Modified oligonucleotides: synthesis and strategy for users. Annu. Rev. Biochem. *67*, 99–134.
4. Ito, Y., Suzuki, A., Kawazoe, N., and Imanishi, Y. (2001). In vitro selection of RNA aptamers carrying multiple biotin groups in the side chains. Bioconjug. Chem. *12*, 850–854.
5. Moor, N.A., Ankilova, V.N., Lavrik, O.I., and Favre, A. (2001). Determination of $tRNA^{Phe}$ nucleotides containing the subunits of *Thermus thermophilus* phenylalanyl-tRNA synthetase by photoaffinity crosslinking. Biochim. Biophys. Acta *1518*, 226–236.
6. Vaish, N.K., Fraley, A.W., Szostak, J.W., and McLaughlin, L.W. (2000). Expanding the structural and functional diversity of RNA: analog uridine triphosphates as candidates for *in vitro* selection of nucleic acids. Nucleic Acids Res. *28*, 3316–3322.
7. Tarasow, T.M., Tarasow, S.L., Tu, C., Kellogg, E., and Eaton, B.E. (1999). Characteristics of an RNA Diels-Alderase active site. J. Am. Chem. Soc. *121*, 3614–3617.
8. Jensen, K.B., Atkinson, B.L., Willis, M.C., Koch, T.H., and Gold, L. (1995). Using *in vitro* selection to direct the covalent attachment of human immunodeficiency virus type 1 Rev protein to high-affinity RNA ligands. Proc. Natl. Acad. Sci. USA *92*, 12220–12224.
9. Gott, J.M., Willis, M.C., Koch, T.H., and Uhlenbeck, O.C. (1991). A specific, UV-induced RNA-protein cross-link using 5-bromouridine-substituted RNA. Biochemistry *30*, 6290–6295.
10. Langer, P.R., Waldrop, A.A., and Ward, D.C. (1981). Enzymatic synthesis of biotin-labeled polynucleotides: novel nucleic acid affinity probes. Proc. Natl. Acad. Sci. USA *78*, 6633–6637.
11. Switzer, C.Y., Moroney, S.E., and Benner, S.A. (1993). Enzymatic recognition of the base pair between isocytidine and isoguanosine. Biochemistry *32*, 10489–10496.
12. Piccirilli, J.A., Krauch, T., Moroney, S.E., and Benner, S.A. (1990). Enzymatic incorporation of a new base pair into DNA and RNA extends the genetic alphabet. Nature *343*, 33–37.
13. Tor, Y., and Dervan, P.B. (1993). Site-specific enzymatic incorporation of an unnatural base, N^6-(6-aminohexyl)isoguanosine, into RNA. J. Am. Chem. Soc. *115*, 4461–4467.
14. Held, H.A., Roychowdhury, A., and Benner, S.A. (2003). C-5 modified nucleosides: Direct insertion of alkynyl-thio functionality in pyrimidines. Nucleosides Nucleotides Nucleic Acids *22*, 391–404.
15. Held, H.A., and Benner, S.A. (2002). Challenging artificial genetic systems: thymidine analogs with 5-position sulfur functionality. Nucleic Acids Res. *30*, 3857–3869.
16. Brown, L.J., May, J.P., and Brown, T. (2001). Synthesis of a modified thymidine monomer for site-specific incorporation of reporter groups into oligonucleotides. Tetrahedron Lett. *42*, 2587–2591.
17. Sakthivel, K., and Barbas, C.F., III. (1998). Expanding the potential of DNA for binding and catalysis: highly functionalized dUTP derivatives that are substrates for thermostable DNA polymerases. Angew. Chem. Int. Ed. Engl. *37*, 2872–2875.
18. Dewey, T.M., Mundt, A.A., Crouch, G.J., Zyzniewski, M.C., and Eaton, B.E. (1995). New uridine derivatives for systematic evolution of RNA ligands by exponential enrichment. J. Am. Chem. Soc. *117*, 8474–8475.
19. Gutierrez, A.J., Terhorst, T.J., Matteucci, M.D., and Froehler, B.C. (1994). 5-Heteroaryl-2′-deoxyuridine analogs. Synthesis and incorporation into high-affinity oligonucleotides. J. Am. Chem. Soc. *116*, 5540–5544.
20. Froehler, B.C., Jones, R.J., Cao, X., and Terhorst, T.J. (1993). Oligonucleotides derived from 5-(1-propynyl)-2′-*O*-allyl-cytidine: synthesis and RNA duplex formation. Tetrahedron Lett. *34*, 1003–1006.
21. Goodchild, J., Porter, R.A., Raper, R.H., Sim, I.S., Upton, R.M., Viney, J., and Wadsworth, H.J. (1983). Structural requirements of olefinic 5-substituted deoxyuridines for antiherpes activity. J. Med. Chem. *26*, 1252–1257.
22. Robins, M.J., and Barr, P.J. (1983). Nucleic acid related compounds. 39. Efficient conversion of 5-iodo to 5-alkynyl and derived 5-substituted uracil bases and nucleosides. J. Org. Chem. *48*, 1854–1862.
23. Cheetham, G.M.T., and Steitz, T.A. (1999). Structure of a transcribing T7 RNA polymerase initiation complex. Science *286*, 2305–2309.
24. Ishikawa, M., Hirao, I., and Yokoyama, S. (2000). Synthesis of 3-(2-deoxy-β-D-ribofuranosyl)pyrimidin-2-one and 2-amino-6-(N,N-dimethylamino)-9-(2-deoxy-β-D-ribofuranosyl)purine derivatives for an unnatural base pair. Tetrahedron Lett. *41*, 3931–3934.
25. Ohtsuki, T., Kimoto, M., Ishikawa, M., Mitsui, T., Hirao, I., and Yokoyama, S. (2000). Unnatural base pairs for specific transcription. Proc. Natl. Acad. Sci. USA *98*, 4922–4925.
26. Fujiwara, T., Kimoto, M., Sugiyama, H., Hirao, I., and Yokoyama, S. (2001). Synthesis of 6-(2-thienyl)purine nucleoside derivatives that form unnatural base pairs with pyrimidin-2-one nucleosides. Bioorg. Med. Chem. Lett. *11*, 2221–2223.
27. Hirao, I., Otsuki, T., Fujiwara, T., Mitsui, T., Yokogawa, T., Okuni, T., Nakayama, H., Takio, K., Kigawa, T., Kodama, K., et al. (2002). An unnatural base pair for incorporating amino acid analogs into proteins. Nat. Biotechnol. *20*, 177–182.
28. Morales, J.C., and Kool, E.T. (1998). Efficient replication between non-hydrogen-bonded nucleoside shape analogs. Nat. Struct. Biol. *5*, 950–954.
29. Matray, T.J., and Kool, E.T. (1999). A specific partner for abasic damage in DNA. Nature *399*, 704–708.
30. Broekman, F.W., and Tendeloo, H.J.C. (1962). The iodination of monohydroxypyridines to monohydroxyiodopyridines. Recueil *81*, 107–111.
31. Mitsui, T., Kitamura, A., Kimoto, M., To, T., Sato, A., Hirao, I., and Yokoyama, S. (2003). An unnatural hydrophobic base pair with shape complementarity between pyrrole-2-carbaldehyde and 9-methylimidazo[(4,5)-b]pyridine. J. Am. Chem. Soc. *125*, 5298–5307.
32. Kimoto, M., Shirouzu, M., Mizutani, S., Koide, H., Kaziro, Y., Hirao, I., and Yokoyama, S. (2002). Anti-(Raf-1) RNA aptamers that inhibit Ras-induced Raf-1 activation. Eur. J. Biochem. *269*, 697–704.
33. Shirouzu, M., Morinaka, K., Koyama, S., Hu, C.-D., Hori-Tamura, N., Okada, T., Kariya, K., Kataoka, T., Kikuchi, A., and Yokoyama, S. (1998). Interactions of the amino acid residue at position 31 of the c-Ha-Ras protein with Raf-1 and RalGDS. J. Biol. Chem. *273*, 7737–7742.
34. Kjems, J., Egebjerg, J., and Christiansen, J. (1998). Laboratory Techniques in Biochemistry and Molecular Biology. Analysis of RNA-Protein Complexes In Vitro. (Amsterdam: Elsevier).
35. Chin, J.W., Martin, A.B., King, D.S., Wang, L., and Schultz, P.G. (2002). Addition of a photocrosslinking amino acid to the genetic code of *Escherichia coli*. Proc. Natl. Acad. Sci. USA *99*, 11020–11024.

36. Horiya, S., Li, X., Kawai, G., Saito, R., Katoh, A., Kobayashi, K., and Harada, K. (2003). RNA LEGO: magnesium-dependent formation of specific RNA assemblies through kissing interactions. Chem. Biol. *10*, 645–654.
37. Jaeger, L., and Leontis, N.B. (2000). Tecto-RNA: one-dimensional self-assembly through tertiary interactions. Angew. Chem. Int. Ed. Engl. *39*, 2521–2524.
38. Winfree, E., Liu, F., Wenzler, L.A., and Seeman, N.C. (1998). Design and self-assembly of two-dimensional DNA crystals. Nature *394*, 539–544.
39. Guo, P. (2002). Structure and function of phi29 hexameric RNA that drives the viral DNA packaging motor: review. Prog. Nucleic Acid Res. Mol. Biol. *72*, 415–472.
40. Petach, H., and Gold, L. (2002). Dimensionality is the issue: use of photoaptamers in protein microarrays. Curr. Opin. Biotechnol. *13*, 309–314.
41. Brody, E.N., Willis, M.C., Smith, J.D., Jayasena, S., Zichi, D., and Gold, L. (1999). The use of aptamers in large arrays for molecular diagnostics. Mol. Diagn. *4*, 381–388.
42. Matulic-Adamic, J., and Beigelman, L. (1997). Synthesis of 3-(β-D-ribofuranosyl)-2-fluoropyridine and 3-(β-D-ribofuranosyl)-pyridin-2-one. Tetrahedron Lett. *38*, 203–206.
43. Kovács, T., and Ötvös, L. (1988). Simple synthesis of 5-vinyl- and 5-ethynyl-2′-deoxyuridine-5′-triphosphates. Tetrahedron Lett. *29*, 4525–4528.